

Real-space representation of the second Chern number

Tsuyoshi Shiina, Fumina Hamano, and Takahiro Fukui
Department of Physics, Ibaraki University, Mito 310-8512, Japan
(Dated: February 21, 2025)

We extend Kitaev's real-space formulation of the first Chern number to the second Chern number and establish a computational framework for its evaluation. To test its validity, we apply the derived formula to the disordered Wilson-Dirac model and analyze its ability to capture topological properties in the presence of disorder. Our results demonstrate that the real-space approach provides a viable method for characterizing higher-dimensional topological phases beyond momentum-space formulations.

I. INTRODUCTION

Topological invariants play a crucial role in characterizing phases of matter beyond the conventional symmetry-breaking paradigm [1, 2]. Among them, the Chern number provides a fundamental classification of topological insulators and superconductors in even-dimensional systems [3–17]. While the first Chern number is well understood and widely utilized in the context of quantum Hall systems and time-reversal symmetry-breaking insulators, the second Chern number has gained attention in higher-dimensional generalizations, such as four-dimensional quantum Hall systems [10, 12, 14, 15], three dimensional pumps [5, 13–15], and the Berry curvature description of generic time-reversal invariant systems [18], etc.

The calculation of topological invariants in real space becomes essential for studying disordered and inhomogeneous systems, where momentum space methods fail. Several real-space methods for computing first Chern numbers have been developed. One approach is to use the twisted boundary condition [19], where the twist angles serve as momenta. Another is the so-called Chern marker method [20], in which derivatives with respect to momenta are represented by position operators. Kitaev's method [21] provides a real-space calculation of the first Chern number by utilizing projectors onto specific subsets of lattice sites, rather than employing position operators. In this approach, the entire lattice is divided into three disjoint regions, and a central role is played by the projectors onto them rather than the position operators. This method has been successfully applied to various models which do not allow simple momentum space calculations [22, 23]. Kitaev's approach has the advantage of being manifestly topological, as it is invariant under the deformation of artificially divided regions.

The rest of this paper is organized as follows. In Sec. II, several useful formulas associated with the spectral projector are summarized. In Sec. III, we review Kitaev's real-space formulation of the first Chern number and its key properties. We also check its effectiveness by applying it to the Wilson-Dirac model in two dimensions. In Sec. IV, we present the extension to the second Chern number and discuss its theoretical foundation. We also apply our formula to the Wilson-Dirac model in four di-

mensions and analyze the numerical results. Finally, in Sec. V, we summarize our findings and outline future research directions.

II. BERRY CONNECTION AND CURVATURE

In this section, we summarize several useful formulas associated with the spectral projectors in order to represent the Chern numbers in higher dimensions [18].

We begin with the Bloch Hamiltonian $\mathcal{H}(q)$ for systems with translational invariance on lattices in $d = 2, 4$, or more generally, $2n$ dimensions, where the Schrödinger equation is given by

$$\mathcal{H}(q)\psi_n(q) = \varepsilon_n(q)\psi_n(q). \quad (1)$$

We assume a gapped ground state composed of M -multiplet wave functions, $\psi(q) \equiv (\psi_1, \psi_2, \dots, \psi_M)$. Using this, we define the Berry connection one-form and the Berry curvature two-form as

$$A = A_\mu dq_\mu, \quad F = dA + A^2 = \frac{1}{2}F_{\mu\nu}dq_\mu dq_\nu, \quad (2)$$

where $A_\mu = \psi^\dagger \partial_\mu \psi$ and $F_{\mu\nu} = (\partial_\mu \psi^\dagger \partial_\nu \psi - \partial_\nu \psi^\dagger \partial_\mu \psi) + [\psi^\dagger \partial_\mu \psi, \psi^\dagger \partial_\nu \psi]$. Throughout this paper, derivatives are taken with respect to momenta, i.e., $\partial_\mu \equiv \partial_{q_\mu}$.

The Berry curvature can be expressed in terms of the spectral projector,

$$P(q) = \psi(q)\psi^\dagger(q), \quad (3)$$

and its exterior derivative with respect to q_μ ,

$$dP = \partial_\mu P dq_\mu. \quad (4)$$

First, note that

$$\psi^\dagger dP = \psi^\dagger (d\psi\psi^\dagger + \psi d\psi^\dagger) = d\psi^\dagger (1 - \psi\psi^\dagger) \equiv d\psi^\dagger \bar{P}, \quad (5)$$

where $\bar{P} \equiv 1 - P$ is the complement of P . Likewise, we have

$$dP\psi = \bar{P}d\psi. \quad (6)$$

On the other hand, since $P^2 = P$, we have $dPP + PdP = dP$, which naturally leads to

$$dP\bar{P} = PdP, \quad dPP = \bar{P}dP. \quad (7)$$

Thus, we obtain

$$[(dP)^2, P] = 0, \quad [(dP)^2, \bar{P}] = 0. \quad (8)$$

Using these, together with Eqs. (5) and (6), we find

$$\begin{aligned} \psi^\dagger (dP)^2 \psi &= d\psi^\dagger \bar{P} d\psi = d\psi^\dagger (1 - \psi\psi^\dagger) d\psi \\ &= d\psi^\dagger d\psi + \psi^\dagger d\psi\psi^\dagger d\psi = F, \end{aligned} \quad (9)$$

which leads to

$$\begin{aligned} F^2 &= \psi^\dagger (dP)^2 \psi \psi^\dagger (dP)^2 \psi = \psi^\dagger (dP)^2 P (dP)^2 \psi \\ &= \psi^\dagger P (dP)^4 \psi. \end{aligned} \quad (10)$$

Applying this repeatedly yields $F^n = \psi^\dagger P (dP)^{2n} \psi$. This expression is useful for representing the Chern numbers in terms of the projector P . Namely, the n th Chern number is given by

$$c_n = \frac{1}{n!} \left(\frac{i}{2\pi} \right)^n \int \text{tr} F^n = \frac{1}{n!} \left(\frac{i}{2\pi} \right)^n \int \text{tr} P (dP)^{2n}. \quad (11)$$

Since P allows a real-space representation, the latter formula serves as a starting point for the real-space formulation of the Chern numbers.

III. FIRST CHERN NUMBER

We review the real-space representation of the first Chern number introduced by Kitaev [21] and establish our notation. This approach can be naturally extended to the second Chern number.

A. The Kitaev formula for the first Chern number

Let us explore how the first Chern number, originally defined in momentum space, can be reformulated in terms of a real-space representation on a lattice. From Eq. (11), the first Chern number is given by

$$c_1 = \frac{i}{2\pi} \int d^2q \epsilon^{\mu\nu} \text{tr} P \partial_\mu P \partial_\nu P. \quad (12)$$

Let $P_{in,jm}$ be the real-space representation of the spectral projector, where i, j represent sites in two dimensions, i.e., $i = (i_1, i_2)$, and n, m represent the internal degrees of freedom in the unit cell, which give rise to the non-Abelian nature of the Berry connection. In what follows, the subscripts n, m will be suppressed for simplicity. Let $(X_\mu)_{ij} \equiv i_\mu \delta_{ij}$ be the site position operator. Then, the key matrix for the real-space representation of

the first Chern number (12) is the following products of the matrices P and X_μ , $(\epsilon^{\mu\nu} P[X_\mu, P][X_\nu, P])$. Its diagonal elements do not depend on the sites if the system has translational invariance, $P_{jl} = P_{j-l}$,

$$\begin{aligned} &(\epsilon^{\mu\nu} P[X_\mu, P][X_\nu, P])_{ii} \\ &= \sum_{j,k} \epsilon^{\mu\nu} P_{i-j}(j_\mu - k_\mu) P_{j-k}(k_\nu - i_\nu) P_{k-i} \\ &= \sum_{j,k} \epsilon^{\mu\nu} P_{-j}(j_\mu - k_\mu) P_{j-k}(k_\nu) P_k, \end{aligned} \quad (13)$$

where in the second line we have replaced $j \rightarrow j + i$ and $k \rightarrow k + i$. This indeed shows that the left-hand-side of the above is independent of i . Translational symmetry also allows the Fourier transformation

$$P_{i-j} = \int_{-\pi}^{\pi} \frac{d^2q}{(2\pi)^2} e^{iq(i-j)} P(q). \quad (14)$$

Then, the above matrix is transformed into

$$(\epsilon^{\mu\nu} P[X_\mu, P][X_\nu, P])_{ii} = \left(\frac{i}{2\pi} \right)^2 \int_{-\pi}^{\pi} d^2q \epsilon^{\mu\nu} P \partial_\mu P \partial_\nu P. \quad (15)$$

Thus we have

$$c_1 = \frac{2\pi}{i} \epsilon^{\mu\nu} \text{tr} P[X_\mu, P][X_\nu, P]_{ii}, \quad (16)$$

where the trace is taken only over the internal degrees of freedom, not over the lattice site i . Note again that the above expression does not depend on the site index i . This formula forms the basis of the Chern marker [20, 24].

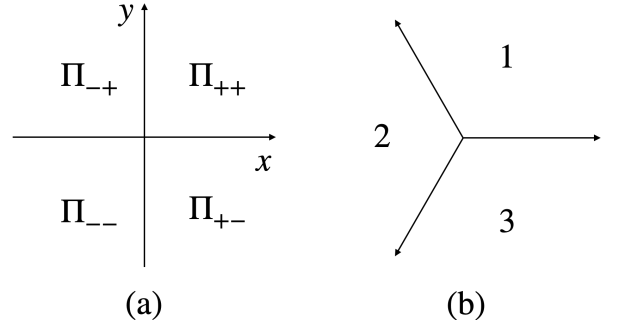


FIG. 1: Regions in the two-dimensional lattice: (a) with respect to $\Pi_x = \Pi_{++} + \Pi_{+-}$ and $\Pi_y = \Pi_{++} + \Pi_{-+}$, and (b) with respect to a generic partition.

Equation (16) can be rewritten into a manifestly topological form [21]. According to Kitaev, let us introduce the lattice projector Π_μ defined by

$$\Pi_\mu = \begin{cases} \delta_{ij} & (i_\mu \geq 0) \\ 0 & (i_\mu < 0) \end{cases} = \theta_{i_\mu} \delta_{ij}, \quad (17)$$

where $\theta_{i_\mu} = 1$ for $i_\mu \geq 0$ and $= 0$ otherwise. Then, we have

$$\begin{aligned} \epsilon^{\mu\nu} \text{tr} P[X_\mu, P][X_\nu, P]_{ii} &= \text{Tr} \epsilon^{\mu\nu} P[\Pi_\mu, P][\Pi_\nu, P] \\ &= \text{Tr} \epsilon^{\mu\nu} P\Pi_\mu P\Pi_\nu P, \end{aligned} \quad (18)$$

where Tr stands for the trace over the sites i as well as the internal degrees of freedom n , $\text{Tr} A = \sum_i \text{tr} A_{ii} = \sum_{i,n} A_{in,in}$. See Refs. [21, 25]. Hence, we reach

$$c_1 = \frac{2\pi}{i} \text{Tr} \epsilon^{\mu\nu} P\Pi_\mu P\Pi_\nu P \equiv \frac{2\pi}{i} \nu_1(P, \Pi_x, \Pi_y) \quad (19)$$

Here, note that Π_x and Π_y have an overlap region $\Pi_x \Pi_y = \Pi_{++}$, where Π_{++} stands for the projector onto $j_x \geq 0$ and $j_y \geq 0$ (See Fig. 1). This overlap region does not contribute to Eq. (19) due to the antisymmetrization in the indices μ, ν . To remove such a contribution, there are two possibilities: One is to replace Π_y with $\Pi_y(1 - \Pi_x)$, and the other is to replace Π_x with $\Pi_x(1 - \Pi_y)$. Namely, one contribution comes through $\nu_1(P, \Pi_{++} + \Pi_{+-}, \Pi_{-+}) = \nu_1(P, \Pi_{++}, \Pi_{-+})$ and the other comes through $\nu_1(P, \Pi_{+-}, \Pi_{++} + \Pi_{-+}) = \nu_1(P, \Pi_{+-}, \Pi_{++})$, each contributing independently,

$$\nu_1(P, \Pi_x, \Pi_y) = \nu_1(P, \Pi_{++}, \Pi_{-+}) + \nu_1(P, \Pi_{+-}, \Pi_{++}). \quad (20)$$

This shows that c_1 is composed of two terms, which are equal, as will be shown below.

Let us divide the two dimensional lattice into three generic regions labeled $A = 1, 2, 3$, as shown in Fig. 1. The corresponding projectors are defined by Π_A . Then, $\sum_A \Pi_A = 1$ and $\Pi_A \Pi_B = \delta_{AB} \Pi_A$ hold. For such a partition of the lattice, we have the following identity,

$$\begin{aligned} \text{Tr} \epsilon^{ABC} P\Pi_A P\Pi_B P\Pi_C &= \text{Tr} \epsilon^{AB} P\Pi_A P\Pi_B P \\ &= \nu_1(P, \Pi_1, \Pi_2), \end{aligned} \quad (21)$$

where we have substituted $\Pi_3 = 1 - \Pi_1 - \Pi_2$ into the left-hand-side of the upper line, and therefore in the right-hand-side, A, B take only 1 and 2. The two terms in Eq. (20) correspond to specific choices of the regions 1 and 2. What is important here is that $\nu_1(P, \Pi_1, \Pi_2)$ is invariant under continuous changes of the regions 1, 2 and 3, which are realized by successively moving one site from one region into another region [21, 25] (see also the proof in four dimensions in Sec. IV). Thus, we have

$$\begin{aligned} c_1 &= \frac{2\pi}{i} 2\nu_1(P, \Pi_1, \Pi_2) \\ &= 2 \frac{2\pi}{i} \text{Tr} \epsilon^{ABC} P\Pi_A P\Pi_B P\Pi_C. \end{aligned} \quad (22)$$

This is the real-space representation derived by Kitaev [21]. Here, the deformation invariance of ν_1 is due to the following conservation law

$$\sum_{i_3} h_{i_1 i_2 i_3} = 0, \quad (23)$$

where h is defined by

$$h_{i_1 i_2 i_3} \equiv \epsilon^{abc} \text{tr} P_{i_a i_b} P_{i_b i_c} P_{i_c i_a}. \quad (24)$$

In Sec. IV, we provide a proof of the deformation invariance in the case of four dimensions.

B. Numerical calculation for the Wilson-Dirac model

In principle, the Kitaev formula is strictly valid only for infinite lattices. When applied to finite systems in numerical computations, it vanishes (See the discussions in [25]). To address this issue, Kitaev proposed a truncation scheme. Specifically, we introduce the following truncation: The lattice sites in each direction μ are assumed to be $-N \leq i_\mu \leq N - 1$ with the periodic boundary condition imposed. Then, introducing the truncation projector $\Pi^{(L)}$ defined by $\Pi^{(L)} \equiv 1$ for $-L \leq i_\mu \leq L - 1$ and $= 0$ otherwise, the Tr operation is modified such that

$$c_1 = 2 \frac{2\pi}{i} \text{Tr} \epsilon^{ABC} \Pi^{(L)} P\Pi_A P\Pi_B P\Pi_C. \quad (25)$$

In what follows, we label the numerical data by the lattice size as well as the truncation size, denoted as (N, L) .

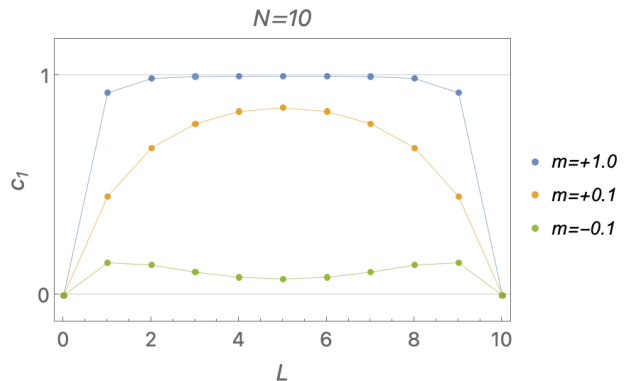


FIG. 2: The truncation size L dependence of the first Chern number c_1 computed for the Wilson-Dirac model using the Kitaev formula. The system size is fixed at $N = 10$ (total sites are $(2N)^2 = 20^2$), and results are shown for $m = 1, 0.1$, and -0.1 , which yield $c_1 = 1, 1$ and 0 , respectively. The other parameters are set $t = b = 1$.

Now, we investigate the Kitaev formula by applying it to the Wilson-Dirac model in $2n$ dimensions ($n = 1$ in this section and $n = 2$ in the next section). To this end, we introduce several notations: Let $j = (j_1, j_2, \dots, j_{2n})$ denote the lattice site in $2n$ dimensions, and let $\hat{\mu}$ be the unit vector in the μ -direction. Then, the Dirac Hamilto-

nian on the lattice with the Wilson term is given by

$$H = -\frac{it}{2} \sum_{\mu=1}^{2n} \gamma^\mu (\delta_\mu - \delta_\mu^{-1}) + m\gamma^{2n+1} + \frac{b}{2} \sum_{\mu=1}^{2n} \gamma^{2n+1} (\delta_\mu + \delta_\mu^{-1} - 2), \quad (26)$$

where γ^μ stands for the γ -matrix in $2n$ dimensions with $\{\gamma^\mu, \gamma^\nu\} = 2\delta^{\mu\nu}$ as well as $\gamma^{2n+1} = (-i)^n \gamma^1 \dots \gamma^{2n}$, and δ_μ is the shift operator in the μ -direction, defined by $\delta_\mu f_j = f_{j+\hat{\mu}}$.

First, we show in Fig. 2 the dependence of the computed c_1 on the truncation size L in Eq. (25). When $L = 0$ or $L = N$, c_1 vanishes. In the case of $L = 0$, this is because everything is truncated out. On the other hand, for $L = N$, implying that nothing is truncated, c_1 also vanishes due to the presence of an artificial boundary at $j_\mu = -N$ and $j_\mu = N - 1$, which cancels with the contributions from the boundary at $j_\mu = 0$. Here, the term ‘‘boundary’’ refers to the interface where the projector Π_μ transitions between 0 and 1. Except for these trivial cases, the Kitaev formula yields nonzero values, although they are no longer exact integers, due to the artificial truncation. Nevertheless, we find that choosing $L \sim N/2$ provides the most accurate results, allowing us to infer the expected Chern numbers. This is quite reasonable, as a similar behavior is observed in the winding number as well [25]. Therefore, we set $L = N/2$ in the following calculations.

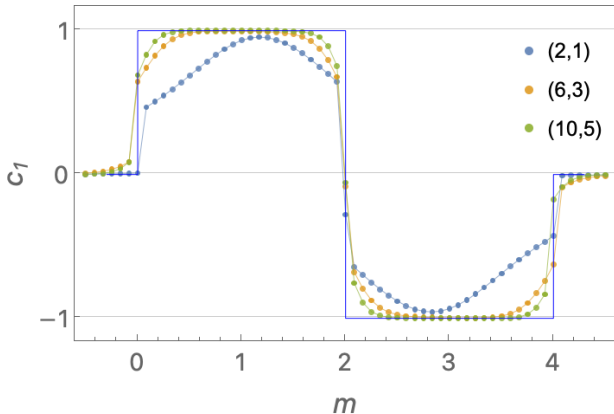


FIG. 3: The first Chern number c_1 as a function of m ($t = b = 1$) computed for the Wilson-Dirac model using the Kitaev formula. The legends indicate the system size and truncation size, (N, L) . The blue lines represent the exact Chern numbers.

In Fig. 3, the first Chern number is plotted as a function of m . A system size of $N = 10$ (totaling 20^2 sites) is sufficient to clearly distinguish the phases of the model. Remarkably, even with a minimal size $N = 2$ (4^2 sites), the Kitaev formula qualitatively captures the phase diagram.

IV. SECOND CHERN NUMBER

So far, we have reviewed the real-space representation of the first Chern number derived by Kitaev. The generalization to the second Chern number is straightforward. In this section, we extend the Kitaev formula to the second Chern number and verify it by applying it to the Wilson-Dirac model.

A. Kitaev formula in four dimensions

From Eq. (11), the second Chern number is given by

$$c_2 = \frac{1}{2!} \left(\frac{i}{2\pi} \right)^2 \int d^4q \epsilon^{\mu\nu\rho\sigma} \text{tr} P \partial_\mu P \partial_\nu P \partial_\rho P \partial_\sigma P. \quad (27)$$

The first step is to Fourier-transform from momentum space to real space. Following the same procedure as in Eq. (15), we obtain

$$\begin{aligned} & \epsilon^{\mu\nu\rho\sigma} \text{tr} P[X_\mu, P][X_\nu, P][X_\rho, P][X_\sigma, P]_{ii} \\ &= \left(\frac{i}{2\pi} \right)^4 \int d^4q \epsilon^{\mu\nu\rho\sigma} \text{tr} P \partial_\mu P \partial_\nu P \partial_\rho P \partial_\sigma P. \end{aligned} \quad (28)$$

The left-hand side does not depend on the site i . The next step is to express the real-space position operator using the lattice projection operator defined in Eq. (17). Specifically, the four-dimensional counterpart of Eq. (18) is given by

$$\begin{aligned} & \text{tr} \epsilon^{\mu\nu\rho\sigma} P[X_\mu, P][X_\nu, P][X_\rho, P][X_\sigma, P]_{ii} \\ &= \text{Tr} \epsilon^{\mu\nu\rho\sigma} P[\Pi_\mu, P][\Pi_\nu, P][\Pi_\rho, P][\Pi_\sigma, P] \\ &= \text{Tr} \epsilon^{\mu\nu\rho\sigma} P \Pi_\mu P \Pi_\nu P \Pi_\rho P \Pi_\sigma P. \end{aligned} \quad (29)$$

Thus, as a generalization of Eq. (19), we obtain the real space representation of the second Chern number,

$$c_2 = \frac{1}{2!} \left(\frac{2\pi}{i} \right)^2 \text{Tr} \epsilon^{\mu\nu\rho\sigma} P \Pi_\mu P \Pi_\nu P \Pi_\rho P \Pi_\sigma P. \quad (30)$$

This formula is sufficiently useful for calculating the second Chern number, the reason for which will be explained shortly.

In the case of the first Chern number, Eq. (19) can be simplified by eliminating overlapping regions and utilizing the deformation invariance of the partition into three regions. Similarly, in the present case, such a simplification is also possible. Specifically, we divide the four-dimensional lattice into five generic regions labeled as $A = 1, \dots, 5$. For a fixed set of five sites i_1, \dots, i_5 , we define

$$h_{i_1 i_2 i_3 i_4 i_5} \equiv \epsilon^{abcde} \text{tr} P_{i_a i_b} P_{i_b i_c} P_{i_c i_d} P_{i_d i_e} P_{i_e i_a}, \quad (31)$$

where a, \dots, e take values from 1 to 5. Then, similarly

to Eq. (21), we have

$$\begin{aligned}\nu_2 &\equiv \sum_{i_1 \in 1} \sum_{i_2 \in 2} \sum_{i_3 \in 3} \sum_{i_4 \in 4} \sum_{i_5 \in 5} h_{i_1 i_2 i_3 i_4 i_5} \\ &= \text{Tr} \epsilon^{ABCDE} P \Pi_A P \Pi_B P \Pi_C P \Pi_D P \Pi_E \\ &= \text{Tr} \epsilon^{ABCD} P \Pi_A P \Pi_B P \Pi_C P \Pi_D P, \end{aligned} \quad (32)$$

where Π_A is the lattice projector onto the region A , and in the last line, A, B, C, D take values 1, 2, 3, and 4 only. As an example of a generic five-partition of the four-dimensional lattice, we can define the following: Starting with $\Pi_1 = \Pi_x$, we take $\Pi_2 = \Pi_y(1 - \Pi_x)$, $\Pi_3 = \Pi_z(1 - \Pi_x)(1 - \Pi_y)$, $\Pi_4 = \Pi_w(1 - \Pi_x)(1 - \Pi_y)(1 - \Pi_z)$, and Π_5 the remaining region $\Pi_5 = (1 - \Pi_x)(1 - \Pi_y)(1 - \Pi_z)(1 - \Pi_w)$. This is one example of partitions of the four dimensional lattice into five regions. Other generic partitions included in (30) can be constructed, for example, by starting with $\Pi_2 = \Pi_y$, then successively removing the overlap regions, $\Pi_1 = \Pi_x(1 - \Pi_y)$, and so on. In this way, we obtain a total of $4!$ generic regions that contribute to Eq. (30).

Moreover, as in the case of the first Chern number, each contribution is the same due to the invariance under deformation of the region. It is guaranteed by the conservation law

$$\sum_{i_5} h_{i_1 i_2 i_3 i_4 i_5} = 0. \quad (33)$$

The invariance can be proved as follows: The spectral projector satisfies $P^2 = P$, which is explicitly expressed by $\sum_{k,l} P_{im,kl} P_{kl,jn} = P_{im,jn}$, where i, k, j stand for the sites while m, l, n denote the internal degrees of freedom. Using this property, we show that summing $h_{i_1 i_2 i_3 i_4 i_5}$ in Eq. (31) over one of i_μ , for instance, summing over i_5 for all sites in the four-dimensional lattice, vanishes:

$$\sum_{i_5} h_{i_1 i_2 i_3 i_4 i_5} = \text{tr} \epsilon^{abcd} P_{i_a i_b} P_{i_b i_c} P_{i_c i_d} P_{i_d i_a} = 0. \quad (34)$$

Now, let us focus our attention on a specific site $i_0 \in 5$, and define region $5' \equiv 5 - \{i_0\}$, where 5 stands for the set of sites in region 5. Then,

$$\nu_2 = h_{12345} = h_{12345'} + h_{1234i_0}, \quad (35)$$

where we have used the shorthand notation, $h_{1i_2 i_3 i_4 i_5} \equiv \sum_{i_1 \in 1} h_{i_1 i_2 i_3 i_4 i_5}$, and so on. If the site i_0 is assigned to region 4, ν_2 changes to

$$\nu_2' = h_{12345'} + h_{123i_0 5'}. \quad (36)$$

Their difference is

$$\nu_2 - \nu_2' = h_{1234i_0} - h_{123i_0 5'}. \quad (37)$$

This actually vanishes. To show this, note that the summation of Eq. (34) over $i_1 \in 1$, $i_2 \in 2$, and $i_3 \in 3$ as well as the assignment $i_4 = i_0$ yield

$$0 = h_{123i_0(1+2+3+4+i_0+5')} = h_{123i_0 4} + h_{123i_0 5'}. \quad (38)$$

This ensures that Eq. (37) indeed vanishes, telling that even if the boundary between the regions 4 and 5 are deformed, ν_2 is invariant. Since $h_{i_1 i_2 i_3 i_4 i_5}$ is antisymmetric with respect to its indices i_1, \dots, i_5 , it turns out that ν_2 is invariant under general deformation of the five regions. Thus, we conclude that

$$c_2 = \frac{4!}{2!} \left(\frac{2\pi}{i} \right)^2 \text{Tr} \epsilon^{ABCDE} P \Pi_A P \Pi_B P \Pi_C P \Pi_D P \Pi_E. \quad (39)$$

This is one of the main results of the paper, i.e., the real space representation of the second Chern number. More generically in $2n$ -dimensions, the n th Chern number can be expressed in real $2n$ dimensional space as

$$\begin{aligned} c_n &= \frac{(2n)!}{n!} \left(\frac{2\pi}{i} \right)^n \\ &\times \text{Tr} \epsilon^{A_1 A_2 \dots A_{2n} A_{2n+1}} P \Pi_{A_1} P \Pi_{A_2} \dots P \Pi_{A_{2n+1}}. \end{aligned} \quad (40)$$

Equations (39) and (40) are important as they demonstrate that higher Chern numbers can also be described using the Kitaev formula. However, even for the second Chern number, where calculations must be performed with a limited number of sites along each axis, the invariance under partitioning into five regions is slightly violated due to the introduction of the truncation projector in the numerical calculations. In such cases, the formula (30) is expected to provide more accurate results than Eq. (39).

B. Application to the Wilson-Dirac model

So far, we have derived the real-space representation of the second Chern number. To verify its validity, we apply it to the Wilson-Dirac model.

In Fig. 4, we present the second Chern number computed using the real-space representation (30) as a function of m . Compared to the first Chern number in two dimensions, the system sizes for the four-dimensional calculations are severely limited, ranging from $N = 2$ (totaling 4^4 sites) to $N = 4$ (8^4 sites). For this reason, we first evaluate the second Chern number using Eq. (30) rather than Eq. (39). In particular, the calculation for the smallest system size, $(N, L) = (2, 1)$, serves as a minimal test case. Despite its small size, the overall behavior of the second Chern number is qualitatively reproduced. For reference, we also show the second Chern number computed using Eq. (39) for this minimal case, indicated by open triangles. As mentioned below Eq. (40), a small deviation from the values obtained via Eq. (30) is observed. We have checked that this deviation decreases as the system size increases. Thus, in practical numerical calculations, Eq. (39) can be used with sufficient accuracy.

The system with $(N, L) = (3, 1)$ is comparable to the system with $(2, 1)$, despite its larger system size. This

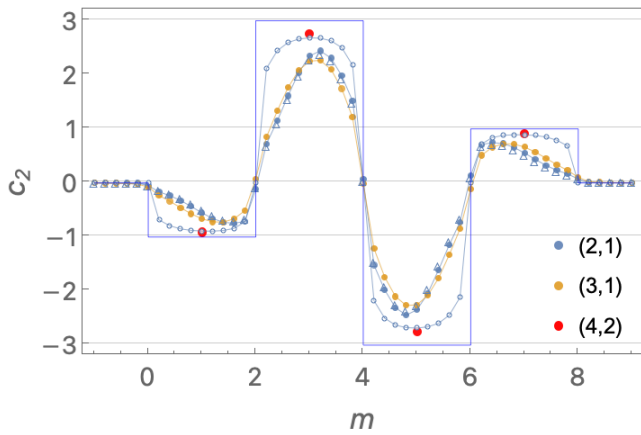


FIG. 4: Second Chern number for the Wilson-Dirac model. Colored connected points represent calculations using the real-space representation (30) with system and truncation sizes $(N, L) = (2, 1)$, $(3, 1)$, and $(4, 2)$, as a function of m , where the other parameters are set $t = b = 1$. For the largest system, $(4, 2)$, results are shown only for four red points at $m = 1, 3, 5, 7$ due to computational cost. Open triangles indicate results for $(2, 1)$ computed using Eq. (39). Connected open small circles correspond to calculations performed in momentum space, where momentum space is discretized into a 12^4 mesh. The blue lines shows the exact second Chern numbers.

is probably because the truncation size L of the former is not the optimal choice, $L = N/2$, as discussed in Sec. III B. Indeed, the system with $(4, 2)$, which satisfies this condition, yields better results.

Next, let us compare the results of the above real-space calculations with those in the conventional momentum space. In the case of the first Chern number, the computational method of the U(1) Berry curvature in a discretized momentum space has been established [26], which is manifestly gauge-invariant and gives strictly integer numbers. However, in the case of the second Chern number, which inevitably involves non-Abelian Berry curvature, no rigorous algorithm for computation in momentum space has been developed so far. Therefore, although the calculation is approximate, let us compare the momentum-space calculations [16] with the present real-space calculations. In Fig. 4, the momentum-space calculations with a 12^4 mesh are shown by small open circles. They yield results similar to those of the real-space calculations with the system size $(N, L) = (4, 2)$. Although the computational cost of the momentum-space calculation is much lower than that of the real-space calculation, the advantage of the latter is that it allows calculations in the presence of disorder in the model.

To investigate this further, we now examine a disordered Wilson-Dirac model. In Eq. (26), we define the model with a uniform kinetic term characterized by the parameter t , and a uniform mass term with the parameter m . We introduce disorder into these parameters, such

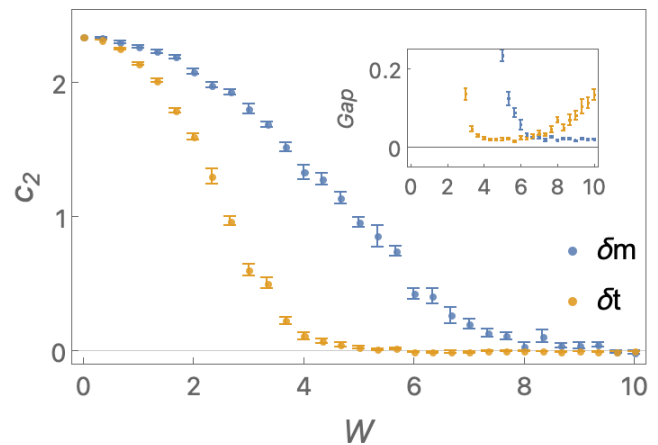


FIG. 5: Ensemble average of the second Chern numbers for the disordered Wilson-Dirac model with sizes $(N, L) = (2, 1)$. Orange dots indicate those of the model with random hopping parameters only, as a function of $W = W_t$ (with $W_m = 0$), whereas the blue dots show those with random mass parameters only, as a function of $W = W_m$ (with $W_t = 0$). The parameters used are $m = 3$, $t = b = 1$. Inset shows the averaged gap at half-filling. Each point shows an average over 10 ensembles.

that $t \rightarrow t + W_t \delta t_{j, \hat{\mu}}$, where $t_{j, \hat{\mu}}$ represents an additional random hopping from site j to site $j + \hat{\mu}$. Similarly, we introduce a random mass term $m \rightarrow m + W_m \delta m_j$, where δm_j is a random mass on site j , for comparing the results in the case of disordered hoppings. We assume that $\delta t_{j, \hat{\mu}}$ is an independent random complex variable within the range of $t_{j, \hat{\mu}} \in [-1, 1]/2 + i[-1, 1]/2$, while δm_j is an independent random real variable within the range of $\delta m_j \in [-1, 1]/2$. The parameters W_t and W_m control the strength of disorder.

In Fig. 5, the second Chern numbers of the disordered Wilson-Dirac model are shown as functions of the disorder strengths W_t and W_m . For the pure model, the second Chern number is $c_2 = 3$ (numerically, $c_2 \sim 2.35$ for this system size; see Fig. 4). In the case of random hopping disorder, the half-filled gap closes as W_t increases, and then reopens at larger W_t . Accordingly, the second Chern number drops to zero, suggesting a topological transition from $c_2 = 3$ to $c_2 = 0$ without intermediate phases such as $c_2 = \pm 1$. Random mass disorder also appears to drive the $c_2 = 3$ phase to a trivial phase. However, the gap remains nearly closed throughout, implying that the large random mass phase is not a trivial phase but rather a gapless phase where the Chern number is ill-defined.

V. SUMMARY AND DISCUSSIONS

The Kitaev formula for the first Chern number provides a topological description of the Chern number in real space. In addition to its conceptual significance, it

is also quite useful for practical computations. In this paper, we first applied the Kitaev formula to the Wilson-Dirac model in two dimensions and explored its utility by testing the truncation scheme to identify the most suitable one. We then generalized the Kitaev formula to the second Chern number and examined its validity. Despite the system size limitations for computations in higher-dimensional space, the second Chern number for the Wilson-Dirac model can be qualitatively reproduced. This opens up possibilities for investigating topological transitions driven by disorder.

In higher dimensions, the computational limitation of the system sizes is severe, so it may be desirable to invent hybrid formulas that are defined partially in real space and partially in momentum space, as a potential future direction. For example, the Thouless pump is defined in 1+1 dimensions, requiring both real space and momentum space, as the time variable can be regarded

as a periodic momentum. Indeed, spatial disorder is random in real space but remains constant in time, making it suitable for treatment in such a hybrid space.

The Wilson-Dirac model shows only two kinds of the first Chern numbers in two dimensions, while in four dimensions it shows four kinds of the second Chern numbers. It would be interesting to explore whether the model exhibits multi-step topological transitions driven by disorder.

Acknowledgments

This work was supported in part by a Grant-in-Aid for Scientific Research (Grant No. 22K03448) from the Japan Society for the Promotion of Science.

-
- [1] M. Z. Hasan and C. L. Kane, *Reviews of Modern Physics* **82**, 3045 (2010), URL <http://link.aps.org/doi/10.1103/RevModPhys.82.3045>.
- [2] X.-L. Qi and S.-C. Zhang, *Reviews of Modern Physics* **83**, 1057 (2011), URL <http://link.aps.org/doi/10.1103/RevModPhys.83.1057>.
- [3] D. J. Thouless, M. Kohmoto, M. P. Nightingale, and M. den Nijs, *Physical Review Letters* **49**, 405 (1982), URL <http://link.aps.org/doi/10.1103/PhysRevLett.49.405>.
- [4] M. Kohmoto, *Annals of Physics* **160**, 343 (1985).
- [5] X.-L. Qi, T. L. Hughes, and S.-C. Zhang, *Physical Review B* **78**, 195424 (2008), URL <http://link.aps.org/doi/10.1103/PhysRevB.78.195424>.
- [6] A. P. Schnyder, S. Ryu, A. Furusaki, and A. W. W. Ludwig, *Physical Review B* **78**, 195125 (2008), URL <http://link.aps.org/doi/10.1103/PhysRevB.78.195125>.
- [7] T. Thonhauser, D. Ceresoli, D. Vanderbilt, and R. Resta, *Physical Review Letters* **95**, 137205 (2005), URL <https://link.aps.org/doi/10.1103/PhysRevLett.95.137205>.
- [8] D. Ceresoli, T. Thonhauser, D. Vanderbilt, and R. Resta, *Physical Review B* **74**, 024408 (2006), URL <https://link.aps.org/doi/10.1103/PhysRevB.74.024408>.
- [9] T. Fukui, T. Fujiwara, and Y. Hatsugai, *Journal of the Physical Society of Japan* **77**, 123705 (2008), <https://doi.org/10.1143/JPSJ.77.123705>, URL <https://doi.org/10.1143/JPSJ.77.123705>.
- [10] H. M. Price, O. Zilberberg, T. Ozawa, I. Carusotto, and N. Goldman, *Physical Review Letters* **115**, 195303 (2015), URL <https://link.aps.org/doi/10.1103/PhysRevLett.115.195303>.
- [11] H. M. Price, O. Zilberberg, T. Ozawa, I. Carusotto, and N. Goldman, *Physical Review B* **93**, 245113 (2016), URL <https://link.aps.org/doi/10.1103/PhysRevB.93.245113>.
- [12] T. Fukui and T. Fujiwara, *Journal of the Physical Society of Japan* **85**, 124709 (2016), URL <http://dx.doi.org/10.7566/JPSJ.85.124709>.
- [13] T. Fukui and T. Fujiwara, *Physical Review B* **96**, 205404 (2017), URL <https://link.aps.org/doi/10.1103/PhysRevB.96.205404>.
- [14] M. Lohse, C. Schweizer, H. M. Price, O. Zilberberg, and I. Bloch, *Nature* **553**, 55 (2018), ISSN 1476-4687, URL <http://dx.doi.org/10.1038/nature25000>.
- [15] O. Zilberberg, S. Huang, J. Guglielmon, M. Wang, K. P. Chen, Y. E. Kraus, and M. C. Rechtsman, *Nature* **553**, 59 (2018), ISSN 1476-4687, URL <http://dx.doi.org/10.1038/nature25011>.
- [16] M. Mochol-Grzelak, A. Dauphin, A. Celi, and M. Lewenstein, *Quantum Science and Technology* **4**, 014009 (2018), URL <https://dx.doi.org/10.1088/2058-9565/aae93b>.
- [17] W. Zhang, F. Di, X. Zheng, H. Sun, and X. Zhang, *Nature Communications* **14**, 1083 (2023), URL <https://doi.org/10.1038/s41467-023-36767-8>.
- [18] Y. Hatsugai, *New Journal of Physics* **12**, 065004 (2010), URL <https://dx.doi.org/10.1088/1367-2630/12/6/065004>.
- [19] Q. Niu, D. Thouless, and Y.-S. Wu, *Physical Review B* **31**, 3372 (1985), URL <http://link.aps.org/doi/10.1103/PhysRevB.31.3372>.
- [20] R. Bianco and R. Resta, *Phys. Rev. B* **84**, 241106 (2011), URL <https://link.aps.org/doi/10.1103/PhysRevB.84.241106>.
- [21] A. Kitaev, *Annals of Physics* **321**, 2 (2006), cond-mat/0506438, URL <http://arXiv.org/abs/cond-mat/0506438>.
- [22] A. Chen, Y. Guan, P. M. Lenggenhager, J. Maciejko, I. Boettcher, and T. c. v. Bzdušek, *Phys. Rev. B* **108**, 085114 (2023), URL <https://link.aps.org/doi/10.1103/PhysRevB.108.085114>.
- [23] Z. F. Osseweijer, L. Eek, A. Moustaj, M. Fremling, and C. Morais Smith, *Phys. Rev. B* **110**, 245405 (2024), URL <https://link.aps.org/doi/10.1103/PhysRevB.110.245405>.
- [24] E. Prodan, *New Journal of Physics* **12**, 065003 (2010), URL <https://dx.doi.org/10.1088/1367-2630/12/6/065003>.
- [25] F. Hamano and T. Fukui, *Phys. Rev. B* **110**,

045437 (2024), URL <https://link.aps.org/doi/10.1103/PhysRevB.110.045437>.

[26] T. Fukui, Y. Hatsugai, and H. Suzuki, Journal of the

Physical Society of Japan **74**, 1674 (2005), URL <http://dx.doi.org/10.1143/JPSJ.74.1674>.